

Optimization and Thermodynamic Studies of Lead (II) and Cadmium (II) Ions Removal from Water Using *Musa acuminata* Pseudo-Stem Biochar

Daniel Nimusiima, Irene Nalumansi, Paul Mukasa, Denis Byamugisha, Emmanuel Ntambi*

Department of Chemistry, Faculty of Science, Mbarara University of Science and Technology, Mbarara, Uganda

Email: *emmantambi@must.ac.ug

How to cite this paper: Nimusiima, D., Nalumansi, I., Mukasa, P., Byamugisha, D. and Ntambi, E. (2023) Optimization and Thermodynamic Studies of Lead (II) and Cadmium (II) Ions Removal from Water Using *Musa acuminata* Pseudo-Stem Biochar. *Green and Sustainable Chemistry*, 13, 254-268.

<https://doi.org/10.4236/gsc.2023.134014>

Received: August 23, 2023

Accepted: November 3, 2023

Published: November 6, 2023

Copyright © 2023 by author(s) and Scientific Research Publishing Inc. This work is licensed under the Creative Commons Attribution International License (CC BY 4.0).

<http://creativecommons.org/licenses/by/4.0/>



Open Access

Abstract

We recently found out that water from the Ugandan stretch of the Kagera transboundary river (East Africa) is contaminated with lead (Pb^{2+}) and cadmium (Cd^{2+}) ions at levels that are above permissible limits in drinking water. Because lignocellulosic biomass-based adsorbents have been explored for the remediation of metal ions from water, this study investigated the potential of *Musa acuminata* pseudo-stem (MAPS) biochar for the remediation of Pb^{2+} and Cd^{2+} ions from water. Batch adsorption experiments were performed to optimize the adsorption conditions while the isotherms were analyzed using Freundlich and Langmuir models. Results showed that the maximum adsorption capacity at equilibrium was 769.23 mg/g and 588.23 mg/g for Pb^{2+} and Cd^{2+} ions, respectively. Langmuir isotherm model provided the best fit for the data, and it was favorable since all r^2 values ($Cd^{2+} = 0.9726$ and $Pb^{2+} = 0.9592$) were close to unity. Gibb's free energy change was found to be negative for both metals, implying the feasibility of the adsorption process. Correspondingly, the enthalpy change was positive for both metal ions which revealed that the adsorption process was endothermic and it occurred randomly at the solid-liquid interface. These results suggested that biochar from MAPs could be utilized for the removal of Pb^{2+} and Cd^{2+} from polluted water in the Kagera transboundary river to make it suitable for domestic use. Further studies should consider chemical modification of the biochar as well as characterization to examine the chemical nature of the biochar.

Keywords

Adsorbent, Biochar, Lignocellulose, Heavy Metals, Water Treatment

1. Introduction

Water is a vital resource for human survival and well-being, but also for economic development and prosperity [1]. Accordingly, access to clean and safe drinking water is considered (from the right to an adequate standard of living under Article 11(1) of the International Covenant on Economic, Social, and Cultural Rights) to be a fundamental human right [2] [3]. This is further enshrined in Sustainable Development Goal 6 (*i.e.*, clean water and sanitation for all). Contamination of water resources by inorganic, legacy, and emerging organic pollutants has led to the deterioration of water quality, nutrient-climate synergized eutrophication, algal blooms, and water insecurity [4] [5].

Water pollution is a regulated activity in developed countries. In developing countries of Africa and Asia, pollution of water resources is less regulated despite the applicable regulatory structures in place. This is particularly disastrous for stagnant water resources such as lakes where legacy and diffuse nutrient pollution may fuel eutrophication and harmful cyanobacterial blooms [6]. We recently found that water from the Ugandan stretch of the Kagera transboundary river (East Africa) is contaminated with lead (Pb^{2+}) and cadmium (Cd^{2+}) ions at levels (0.023 to 0.043 mg/L and 0.0033 to 0.0101 mg/L) that are above permissible limits in drinking water [7]. For the remediation of these inorganic ions, we opted to explore a potential adsorbent that is locally available (*Musa acuminata* pseudo-stem). Lignocellulosic biomass-based adsorbents have been used for the remediation of metal ions from water [8].

Musa acuminata Colla (*M. acuminata* henceforth) is a banana species that is native to Southern Asia and one of the earliest plants that were domesticated in human history [9]. It has since been introduced and cultivated in different parts of the world [10] [11]. It is an evergreen tree-like perennial plant with a trunk (known as the pseudo stem) composed of packed layers of leaf sheaths emerging from completely or partially buried corm. This part of *M. acuminata* is usually disposed of as organic waste or used in the garden [12]. To achieve optimum removal of the ions, the conditions which affect adsorption were individually investigated.

2. Materials and Methods

2.1. Biochar Preparation

Mature *Musa acuminata* (Enyeru variety) pseudo stems were collected on 15/03/2023 after harvesting fruits from them in Kikagati town council, Isingiro District, Uganda. The collected sheath material was washed with deionized water and thereafter cut into small pieces (2×2 cm) using a stainless-steel knife. They were dried at room temperature (25°C) before grinding into fine powder. Biochar was prepared by heating the dry powder in an oven at 100°C with limited oxygen.

2.2. Adsorption Experiments

Batch experiments were carried out by adding 1 g of the biochar into a 250 ml

Erlenmeyer flask containing 50 ml of different aqueous solutions (5, 10, 15, 20, 25, 30, 35, 40, 45, and 50 mg/l) of lead and cadmium nitrates at different conditions. The conditions varied were: biochar dose (0.2, 0.4, 0.6, 0.8, 1.0, 1.2, 1.4 and 1.6 g), pH (1, 2, 3, 4, 5, 6, 7, 8 and 9), contact time (15, 30, 45, 55, 60, 75, 90 105 and 120 minutes) and temperature (25°C, 30°C, 35°C, 40°C, 45, 50°C, 55°C, 60°C and 65°C). Agitation was done at 150 revolutions per minute (rpm) for one hour at 25°C on a horizontal shaker for sorption equilibrium to occur.

After adsorption, the adsorbent was separated from the solution by filtration through a Whatman (0.45 µm) filter paper. The residual concentration of each metal in the equilibrium solutions (filtrates) was determined. Each treatment was done three times. The percentage removal of each heavy metal was calculated using Equation (1).

$$\text{Adsorption (\%)} = \frac{C_i - C_e}{C_i} \times 100 \quad (1)$$

where C_i and C_e are the initial and residual concentrations of the heavy metal ion at equilibrium [13].

2.3. Metal Concentration Determination by Atomic Absorption Spectrometry

The residual concentration of the two ions was determined using a flame atomic absorption spectrophotometer (Agilent 240AA, Agilent Technologies, Santa Clara, California, USA) at the respective 283.3 nm and 228.8 nm for Pb and Cd. The actual heavy metal concentrations were determined from calibration curves constructed from diluted working standards of 1000 ppm stock solutions of nitrate and chloride salts of the metals. The linearity of the calibration curves was checked, and these were within acceptable limits ($r^2 > 0.9950$ in all cases). Further, the quality of instrumental results was guaranteed through analysis of procedural blanks and spiked samples, whose recoveries (range: 97.9% to 101.5%) were analytically considered acceptable. Relative Standard Deviations of the experiments (analytical precision) ranged between 3.7% and 4.9%.

2.4. Adsorption Isotherms

In adsorption studies, the equilibrium retention of the adsorbate onto the adsorbent is better described by mathematical models hinged on some assumptions relating to the coverage type, homogeneity, and heterogeneity of the solid surface, as well as the interaction between adsorbate species [14]. These models, which are otherwise termed adsorption isotherms, can explain the probable mechanism of adsorption. In this study, equilibrium data were analyzed using the Langmuir and Freundlich isotherms [15].

Freundlich adsorption isotherm (model) works on the assumption that the adsorption of metal ions occurs on heterogeneous multilayer surfaces with different energy affinities. It is described by Equation (2), proposed by Freundlich in the first instance [16].

$$Q_e = K_f C_e^{1/n} \quad (2)$$

where K_f and n are Freundlich isotherm constants, which depend on the nature of the adsorbent at a given temperature.

Linearizing the equation, the Freundlich equation becomes (Equation (3))

$$\log Q_e = \frac{1}{n} \log C_e + \log K_f \quad (3)$$

where the intercepted $\log K_f$ gives the measure of adsorption capacity (distribution coefficient) and the slope ($\frac{1}{n}$) gives the intensity of adsorption. The variable

Q_e is the amount of metal ion adsorbed at equilibrium (mg/g) and C_e is the concentration of the adsorbate at equilibrium (mg/g) in the solution [16]. In other words, the value of K_f increases with adsorption intensity and that of n is directly related to adsorption greaterity *i.e.*, $1 \leq n \leq 10$ indicates that the adsorption process is favorable [17].

A plot of $\ln Q_e$ against $\ln C_e$ for each metal under investigation was also made and analyzed independently. A plot that obeys Freundlich isotherm gives a straight line with slope ($\frac{1}{n}$) [16].

Langmuir model is based on the assumption that all adsorption sites are of homogenous surface on monolayer and independent of whether active sites are occupied or not. The linear Langmuir equation is given by Equation (4) [18].

$$\frac{C_e}{Q_e} = \frac{1}{Q_{\max}} C_e + \frac{1}{Q_{\max} K_L} \quad (4)$$

where C_e = equilibrium metal ion concentration (mg/l), Q_e = amount of adsorbate adsorbed per unit mass of adsorbent (mg/g), Q_{\max} = maximum adsorption capacity of adsorbent and K_L is the Langmuir constant.

A plot of $\frac{C_e}{Q_e}$ against C_e for each metal under investigation was made and analyzed independently. A plot that obeys Langmuir isotherm gives a straight line with slope $\frac{1}{Q_{\max}}$. Separation factor (R_L) was evaluated by using Equation (5) [14].

$$R_L = \frac{1}{1 + K_L C_o} \quad (5)$$

where K_L = Langmuir constant and C_o = original concentration. The value of R_L indicates whether adsorption is favorable or not and where, unfavorable ($R_L > 1$), linear ($R_L = 1$), favorable ($0 < R_L < 1$), or irreversible ($R_L = 0$) [19].

2.5. Thermodynamic Studies

Adsorption is a temperature-dependent process, and it is vital to perform thermodynamic studies to establish the feasibility and spontaneity of adsorption kinetics [20]. Thermodynamic study of the metal ions adsorption onto biochar from *M. acuminata* pseudo-stem biochar was performed at 293, 303, 308, 313,

318, and 323 K. The equilibrium constant K_c of adsorption was calculated using Equation (6).

$$K_c = \frac{C_a}{C_e} \quad (6)$$

where K_c is the equilibrium sorption distribution coefficient, C_a is the amount of metal ions adsorbed on the biochar at a given temperature and C_e is the metal ion concentration in the solution at equilibrium.

The K_c values obtained were used to determine Gibb's free energy change (ΔG°), enthalpy change (ΔH°), and entropy change (ΔS°) for adsorption of Pb^{2+} and Cd^{2+} ions on MAPS given by Equations (7) and (8).

$$\Delta G^\circ = -RT \log K_c \quad (7)$$

$$\log K_c = \frac{-\Delta H^\circ}{R} \frac{1}{T} + \frac{\Delta S^\circ}{R} \quad (8)$$

where ΔG° is the free energy change of adsorption, R is the universal gas constant ($8.314 \text{ J}\cdot\text{mol}^{-1}\cdot\text{K}^{-1}$) and T is the absolute temperature in Kelvins. The K_c can be expressed in terms of the ΔG° and ΔS° as a function of temperature as given by the van Hoff's reaction isotherm (Equation (8)) [21].

3. Results

3.1. Optimized Adsorption Conditions

3.1.1. Effect of Contact Time

The highest percentage removal of Pb^{2+} and Cd^{2+} ions were 88.1% and 87.2%, respectively (Figure 1) while keeping other parameters constant (pH = 4, 1.0 g biochar dosage, $V = 50 \text{ ml}$, $T = 25^\circ\text{C}$ and $C_0 = 10 \text{ mg/l}$). Beyond 55 minutes and 60 minutes, there was no further increase in the adsorption for Pb^{2+} and Cd^{2+} ions.

3.1.2. Effect of Solution pH

In adsorption, the pH of a solution is an important parameter that provides suitable conditions for maximum adsorption at the adsorbent surface. In this study, adsorption of the ions by MAPS biochar initially increased with an increase in pH up to pH = 4 for Pb^{2+} and pH = 5 for Cd^{2+} . After this, the adsorption was seen to decrease (Figure 2). The highest percentage of removal achieved was 85.1% and 81.0%, respectively.

3.1.3. Effect of Solution Temperature

For solution temperature, the highest percentage of removal was 88.9% (at 45°C) and 79.5% (at 50°C) for Pb^{2+} and Cd^{2+} ions, respectively (Figure 3). There was an initial increase in adsorption with an increase in temperature.

3.1.4. Effect of Adsorbent Dosage

There was a noticeable increase in the removal of Pb^{2+} and Cd^{2+} ions with increasing biochar dosage until an optimum dosage of 1g was reached (Figure 4). The highest adsorption was 80.0% and 77.9%, respectively.

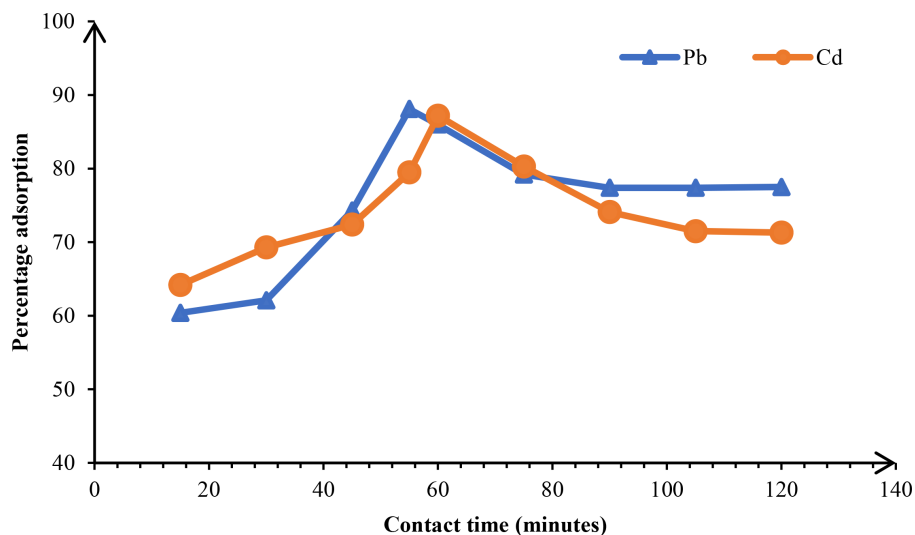


Figure 1. Effect of contact time on the adsorption of lead (II) and cadmium (II) ions from aqueous solution using MAPS biochar.

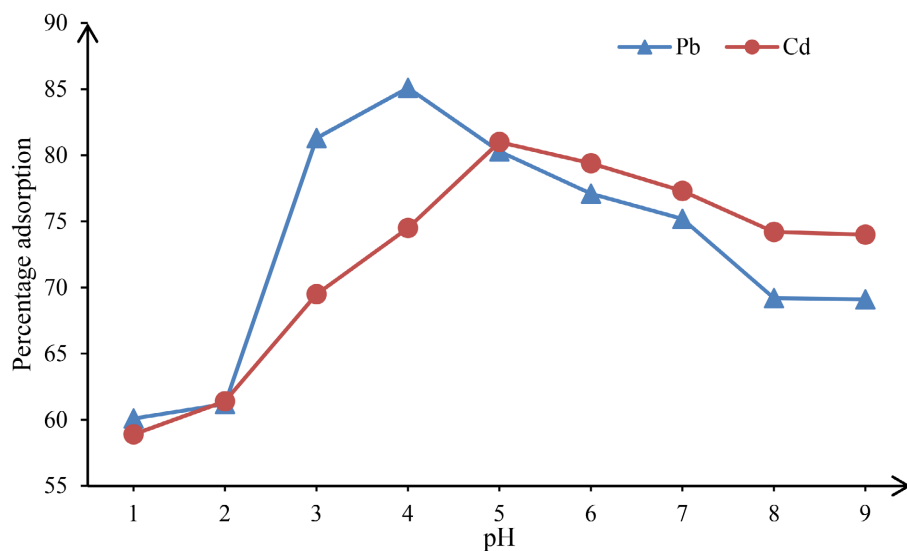


Figure 2. Effect of pH on the adsorption of lead (II) and cadmium (II) ions from aqueous solution using MAPS biochar.

3.1.5. Effect of Initial Metal Ion Concentration

The adsorption of Pb^{2+} and Cd^{2+} ions in this study was observed to decrease with an increment in the initial metal ion concentration from 87.12% to 31.5% and 79.21% to 24.6%, respectively (Figure 5).

3.2. Sorption and Adsorption Isotherms

A Freundlich linear equation was used to obtain sorption and desorption isotherms, and standard multiple linear regression analysis was used to find the best-fit isotherm. The plots of $\ln Q_e$ against $\ln C_e$ for Pb^{2+} and Cd^{2+} ions are depicted in Figure 6 and Figure 7, respectively. Each case obeyed Freundlich isotherm giving a straight line with slope $1/n$, so n for Pb^{2+} was 0.309 ($r^2 = 0.8869$)

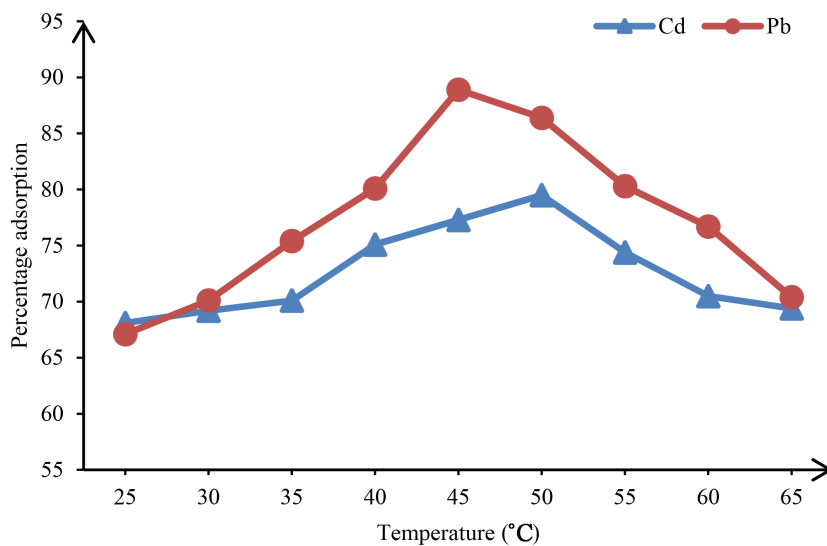


Figure 3. Effect of temperature on the adsorption of lead (II) and cadmium (II) ions from aqueous solution using MAPS biochar.

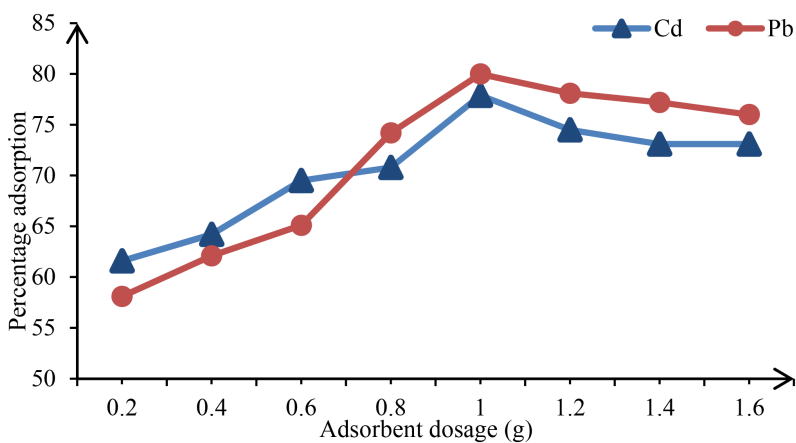


Figure 4. Effect of initial adsorbent dosage on the adsorption of lead (II) and cadmium (II) ions from aqueous solution using MAPS biochar.

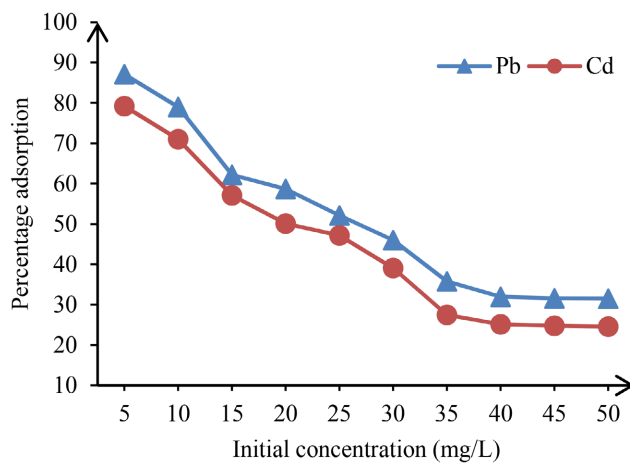


Figure 5. Effect of initial metal ion concentration on the adsorption of lead (II) and cadmium (II) ions from aqueous solution using MAPS biochar.

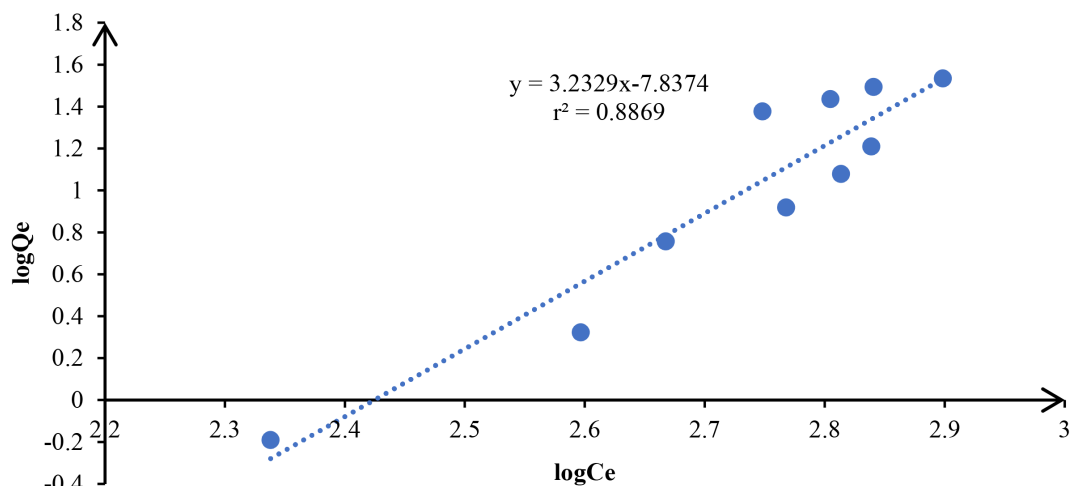


Figure 6. Freundlich adsorption isotherm for the adsorption of lead (II) ions from aqueous solution using MAPS biochar.

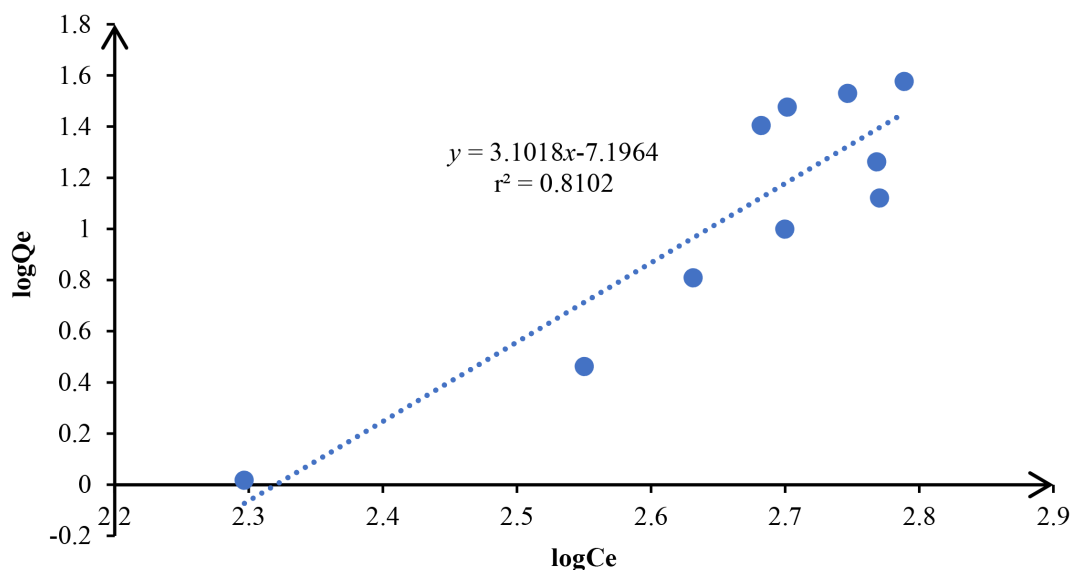


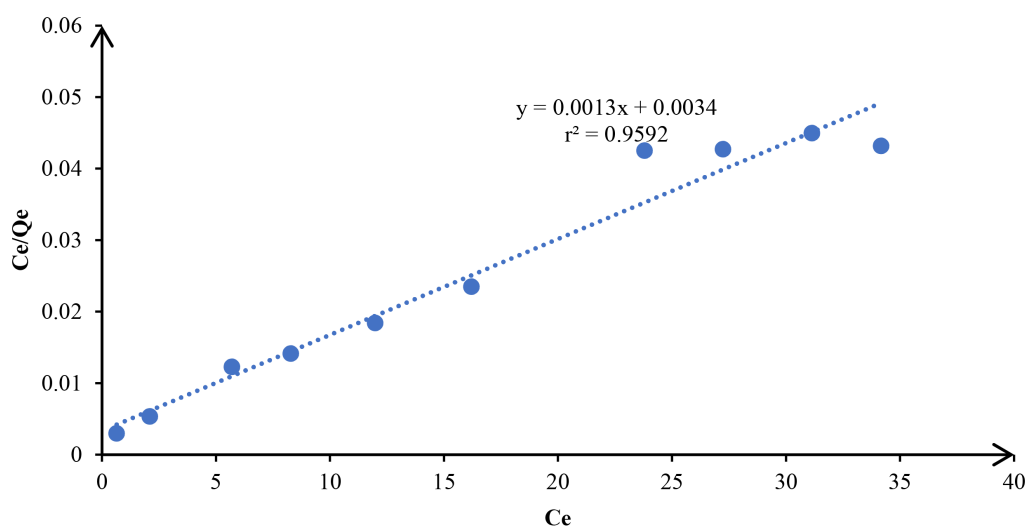
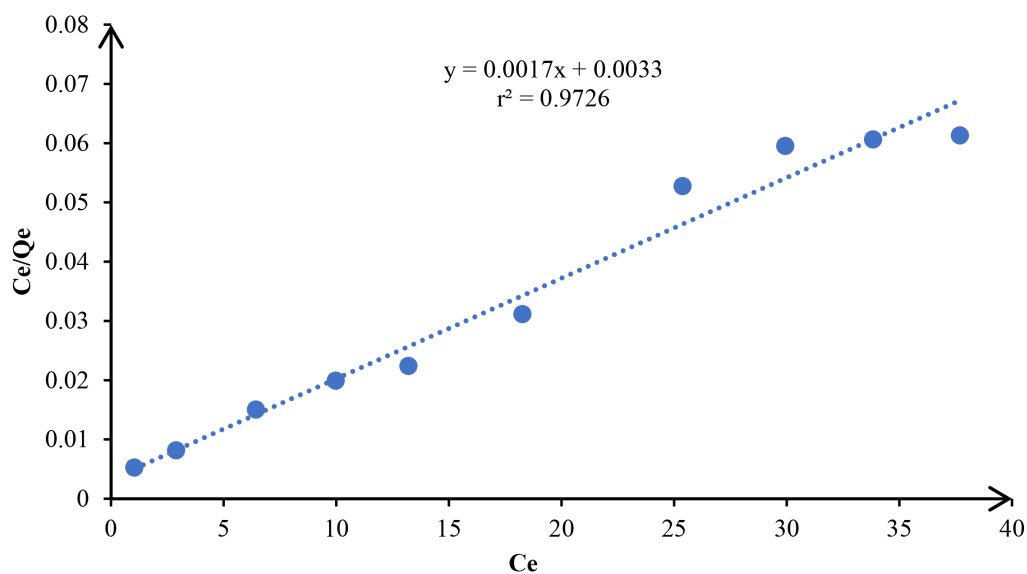
Figure 7. Freundlich adsorption isotherm for the adsorption of cadmium (II) ions from aqueous solution using MAPS biochar.

and for Cd^{2+} ions was 0.322 ($r^2 = 0.8102$) with calculated K_f values of 1.455×10^{-8} mg/g and 6.362×10^{-8} mg/g (**Table 1**). The model explains the values of $n = 1$, linear, $n < 1$, chemical adsorption process ($n > 1$), and physical adsorption process.

Similarly, the Langmuir linear equation was considered, and plots of $\frac{C_e}{Q_e}$ against C_e for Pb^{2+} and Cd^{2+} ions are given in **Figure 8** and **Figure 9**. The plotted graphs obeyed the Langmuir isotherm with a straight line whose slope was $\frac{1}{Q_{\max}}$, so $Q_{\max} = 769.23$ mg/g and 588.23 mg/g for Pb^{2+} and Cd^{2+} ions, respectively (**Table 1**). The straight line confirmed monolayer formation on active sites. From the present study, the coefficient values of $r^2 = 0.9592$ and 0.9726 for

Table 1. Freundlich and Langmuir adsorption isotherm parameters for the adsorption of lead (II) ions and cadmium (II) ions from aqueous solution using MAPS biochar.

Metal ion	Freundlich		Langmuir		
	r^2	n	r^2	Q_{\max} (mg/g)	R_L
Pb ²⁺	0.8869	0.309	0.9592	769.23	0.207
Cd ²⁺	0.8102	0.322	0.9726	588.23	0.162

**Figure 8.** Langmuir adsorption isotherm for the adsorption of lead (II) ions from aqueous solution using MAPS biochar.**Figure 9.** Langmuir adsorption isotherm for the adsorption of cadmium (II) ions from aqueous solution using MAPS biochar.

Pb²⁺ and Cd²⁺ ions, respectively (**Table 1**) and this proved that the Langmuir isotherm model was the most suitable and favorable for the adsorption of the ions in the batch experiments using MAPS biochar as adsorbent material [14].

This was in agreement with the suggestion of the Langmuir isotherm model that adsorption occurred over homogenous surfaces on free active sites. The separation factor (R_L) was found to be 0.207 and 0.162 for Pb^{2+} and Cd^{2+} ions, suggesting that adsorption was favorable for Langmuir isotherm model for both metal ions.

3.3. Thermodynamic Studies

The values of ΔH° and ΔS° for both metal ions were positive (Table 2), and were obtained from slopes and intercepts of the plot of $\log K_c$ against $1/T$ (Figure 10). The calculated thermodynamic values of ΔG° were negative, and this decreased further with an increase in temperature (Table 2).

Table 2. Thermodynamic parameters for adsorption of Pb^{2+} and Cd^{2+} ions from aqueous solution using MAPS biochar.

T (K)	K_c		$1/T$ (K^{-1})	$\log K_c$		ΔG° (Jmol^{-1})		ΔH° (Jmol^{-1})		ΔS° ($\text{JK}^{-1}\cdot\text{mol}^{-1}$)	
	Pb	Cd		Pb	Cd	Pb	Cd	Pb	Cd	Pb	Cd
298	2.0395	2.1348	0.0034	0.3095	0.3294	-766.87	-816.00				
303	2.3445	2.2468	0.0033	0.3700	0.3516	-932.20	-885.62				
308	3.0650	2.3445	0.0033	0.4864	0.3700	-1245.62	-947.58	19142.99	8872.7	66.52	32.27
313	4.0251	3.0161	0.0032	0.6048	0.4794	-1573.81	-1247.6				
318	8.0090	3.4053	0.0032	0.9036	0.5322	-2388.93	-1406.9				
323	6.3529	3.8780	0.0031	0.8030	0.5886	-2156.33	-1580.6				

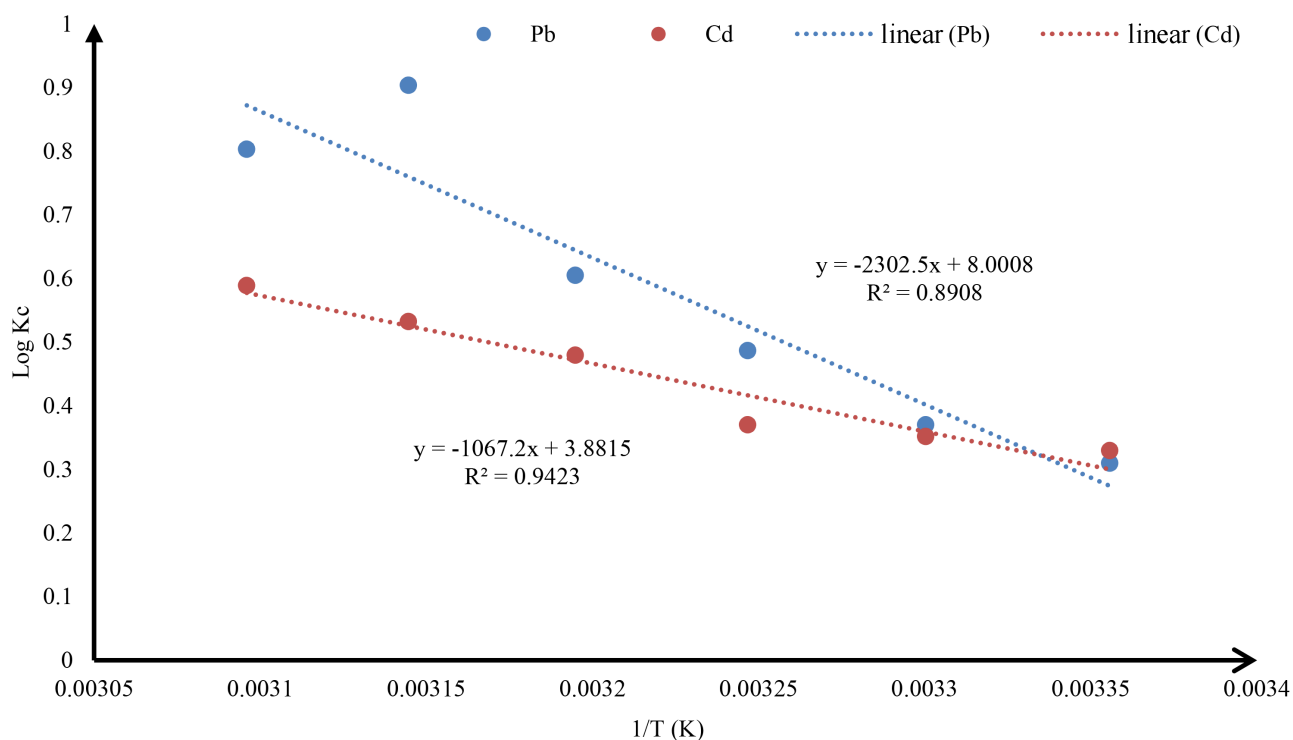


Figure 10. A graph of $\log K_c$ against $1/T$.

4. Discussion

4.1. Optimized Adsorption Parameters

This study recorded increased adsorption of both metal ions with an increase in contact time probably due to the availability of many vacant sites which provided a large surface area for more ions to get adsorbed onto the biochar active sites [15] [22]. Beyond 55 minutes and 60 minutes, there was no further increase in the adsorption for Pb^{2+} and Cd^{2+} ions due to the equilibrium set by the already adsorbed metal ions still in solution. Saturation of free active biochar sites and repulsion of molecules in the solid phase resulted in a percentage decrease in the adsorption of metal ions with contact time [23] [24].

For solution pH, the initial increment in adsorption of the metal ions could be explained by the decrease in competition of metal ions due to the formation of soluble negative metal complexes on active sites of the biochar [25]. This may be due to an increase in the electrostatic binding capacity of metal ions with active sites of the biochar [20]. As pH increases, fewer protons are released which in turn increases charge density around the active sites of biochar and this increases attractive forces of metal ions towards the active sites of the biochar. The low adsorption percentages at low pH were due to protonation of hydronium ions and this creates repulsive forces between metal ions and free active sites of the biochar which hinders the metal ions binding capacity with functional groups on the biochar surface [26].

In examining the effect of initial temperature, there was an initial increase in adsorption with an increase in temperature. This could be explained by an increase in the kinetic energy of the ions in the solution. There was more diffusion of metal ions into the abundant active sites existing on the biochar as temperature increased since diffusion is an endothermic process. Hence, an increase in solution temperature would result in the enlargement of biochar pore size due to activated diffusion triggering them to widen and create more surface for adsorption [20]. Apart from temperature as a factor, hydration ionic radius also affects the adsorption of metal ions on biochar *i.e.*, a smaller hydration ionic radius leads to greater penetration into the pores of the biochar hence better adsorption. In this study, Pb^{2+} (0.401 nm) was adsorbed more than Cd^{2+} (0.426 nm), probably due to the weakening of adsorptive forces of attraction and the reduced number of active sites. This result is in agreement with a previous study using biochar of *Ficus natalensis* fruit which recorded maximum adsorption of 98.4% for Pb^{2+} at 45°C adsorption [20].

There was a noticeable increase in the removal of Pb^{2+} and Cd^{2+} ions with increasing biochar dosage until an optimum dosage of 1 g was reached (Figure 4). The highest adsorption was 80.0% and 77.9%, respectively. The gradual increase in adsorbed ions is because the increase in the amount of adsorbent dosage leads to increased probabilities of the ions getting into contact with the available active adsorption sites of the biochar (increase in surface area) [15] [27]. The decrease in adsorption beyond the adsorbent dosage of 1 mg/l could have been due to the

shielding effect from precipitation of metal hydroxides and already adsorbed metal ions on active sites of the biochar or creation of excess unoccupied sites on the biochar [28]. A previous study also indicated the effects of dosage levels (1 g to 4 g) of biochar of rice husks to cause adsorption of 78.46% and 92.63% Pb^{2+} and Cd^{2+} ions [26], which aligns with our present results.

The adsorption of Pb^{2+} and Cd^{2+} ions in this study was observed to decrease with an increment in the initial metal ion concentration (Figure 5). At low initial concentrations of metal ions, the increase in metal ion adsorption percentages was due to the availability of free active sites of biochar, which enabled greater interaction of the metal ions with the biochar. As the concentration increased, the lower adsorption percentages were caused by the saturation of the adsorption sites on the biochar [29] [30] [31] [32]. As expected, the percentage of Pb^{2+} ions adsorbed was higher than that of Cd^{2+} , possibly due to differences in their ionic charge densities [20].

4.2. Sorption and Adsorption Isotherms

From this study, results showed that it was more favorable for Pb^{2+} and Cd^{2+} ions under the Langmuir isotherm model than Freundlich because the r^2 values obtained were close to 1, and values of n were less than 1 which indicated that adsorption was chemical. This was in agreement with the results obtained by Sobh *et al.* [33] where adsorption of Pb^{2+} ions by *Cymbopogon citratus* was chemical since the value of n obtained was 0.76 less than one. High values of n show a uniform surface on the adsorbent material and low values of n show high adsorption and the presence of high-energy active sites on the adsorbent material as explained by the Freundlich isotherm model.

4.3. Thermodynamic Studies

The values of ΔH° and ΔS° for both metal ions (Table 2) were positive, indicating the irreversibility adsorption of the metal ions onto MAPS biochar. That is, the process is endothermic and favorable [15] [21]. The negative values of ΔG° decreased with an increase in temperature. This indicated the feasibility of the adsorption process and affinity of the biochar for Pb^{2+} and Cd^{2+} ions from water solution.

5. Conclusion

We assessed the feasibility of using MAPS biochar in the remediation of Pb^{2+} and Cd^{2+} ions from water. The obtained results indicated that the maximum adsorption capacity at equilibrium was 769.23 mg/g and 588.23 mg/g for Pb^{2+} and Cd^{2+} ions, respectively. Langmuir isotherm model provided the best fit for the data, and it was favorable since all r^2 values ($\text{Cd}^{2+} = 0.9726$ and $\text{Pb}^{2+} = 0.9592$) were close to unity. The Gibb's free energy change was found to be negative for both metals implying the feasibility of the adsorption process. Correspondingly, the enthalpy change was positive for both metal ions which revealed that the ad-

sorption process was endothermic and it occurred randomly at the solid-liquid interface. These results suggested that biochar from MAPs could be utilized for the removal of Pb²⁺ and Cd²⁺ from polluted water in the Kagera transboundary river to make it suitable for domestic use. Further studies should consider chemical modification of the biochar as well as characterization to examine the chemical nature of the biochar.

Acknowledgements

We are grateful to Timothy Omara for his support in the drafting and proofreading of this article.

Conflicts of Interest

The authors declare no conflicts of interest regarding the publication of this paper.

References

- [1] United Nations (2023) Water “Vital to Human Survival, Economic Development, Prosperity of Every Nation”, Says Secretary-General in Message for World Day Observance. <https://press.un.org/en/2023/sgsm21727.doc.htm#:~:text=Water%20is%20the%20lifeblood%20of,and%20prosperity%20of%20every%20nation>
- [2] Fantini, E. (2020) An Introduction to the Human Right to Water: Law, Politics, and beyond. *Wires Water*, **7**, e1405. <https://doi.org/10.1002/wat2.1405>
- [3] United Nations (2010) About Water and Sanitation. <https://www.ohchr.org/en/water-and-sanitation/about-water-and-sanitation#:~:text=On%2028%20July%202010%2C%20the,RES%2F64%2F292>
- [4] Boretti, A. and Rosa, L. (2019) Reassessing the Projections of the World Water Development Report. *npj Clean Water*, **2**, Article No. 15. <https://doi.org/10.1038/s41545-019-0039-9>
- [5] Li, J., Yang, J., Liu, M., Ma, Z., Fang, W. and Bi, J. (2022) Quality Matters: Pollution Exacerbates Water Scarcity and Sectoral Output Risks in China. *Water Research*, **224**, Article ID: 119059. <https://doi.org/10.1016/j.watres.2022.119059>
- [6] Lürling, M. and Mucci, M. (2020) Mitigating Eutrophication Nuisance: In-Lake Measures Are Becoming Inevitable in Eutrophic Waters in the Netherlands. *Hydrobiologia*, **847**, 4447-4467. <https://doi.org/10.1007/s10750-020-04297-9>
- [7] Nimusiima, D., Byamugisha, D., Omara, T. and Ntambi, E. (2023) Physicochemical and Microbial Quality of Water from the UGANDAN stretch of Kagera Transboundary River. *Limnological Review*, **23**. (In Press)
- [8] Nwagbara, V., Sika, F., Iyama, W., Chigayo, K. and Kwaambwa, H. (2022) Evaluating the Potential Effectiveness of *Moringa oleifera* Seeds Biomass as an Adsorbent in the Removal of Copper (Cu) in Water. *Journal of Geoscience and Environment Protection*, **10**, 120-143. <https://doi.org/10.4236/gep.2022.103010>
- [9] Mathew, N.S. and Negi, P.S. (2017) Traditional Uses, Phytochemistry and Pharmacology of Wild Banana (*Musa acuminata Colla*): A Review. *Journal of Ethnopharmacology*, **196**, 124-140. <https://doi.org/10.1016/j.jep.2016.12.009>
- [10] Yadav, A. (2021) Banana (*Musa acuminata*): The Most Popular and Common In-

- dian Plant with Multiple Pharmacological Potentials. *World Journal of Biology Pharmacy and Health Sciences*, **7**, 36-44.
<https://doi.org/10.30574/wjbphs.2021.7.1.0073>
- [11] Mubarak, S., Suwali, N., Suminar, E. and Kamaluddin, N. (2019) 1-Methylcyclopropene as an Effective Ethylene Inhibitor to Extend *Musa acuminata* Colla "Muli" Postharvest Quality. *IOP Conference Series: Earth and Environmental Science*, **334**, Article ID: 012051. <https://doi.org/10.1088/1755-1315/334/1/012051>
- [12] Salazar, D., Arancibia, M., Casado, S., Viteri, A., López-Caballero, M.E. and Montero, M.P. (2021). Green Banana (*Musa acuminata* AAA) Wastes to Develop an Edible Film for Food Applications. *Polymers*, **13**, Article 3183.
<https://doi.org/10.3390/polym13183183>
- [13] Wang, J., Sun, C., Huang, Q., Chi, Y. and Yan, J. (2021). Adsorption and Thermal Degradation of Microplastics from Aqueous Solutions by Mg/Zn Modified Magnetic Biochars. *Journal of Hazardous Materials*, **419**, Article ID: 126486.
<https://doi.org/10.1016/j.jhazmat.2021.126486>
- [14] Benzaoui, T., Selatnia, A. and Djabali, D. (2018) Adsorption of Copper (II) Ions from Aqueous Solution Using Bottom Ash of Expired Drugs Incineration. *Adsorption Science & Technology*, **36**, 114-129. <https://doi.org/10.1177/0263617416685099>
- [15] Pagala, B. (2023) Characteristic Evaluation of Tamarind Flower Biomass for Mercury Biosorption: A Statistical Approach. *Biomass Conversion and Biorefinery*.
<https://doi.org/10.1007/s13399-023-03769-x>
- [16] Freundlich, H.M. (1906) Over the Adsorption in Solution. *Journal of Physical Chemistry A*, **57**, 385-470. <https://doi.org/10.1515/zpch-1907-5723>
- [17] Chantawong, V., Harvey, N. and Bashkin, V. (2003) Comparison of Heavy Metal Adsorptions by Thai Kaolin and Ballclay. *Water Air and Soil Pollution*, **148**, 111-125.
<https://doi.org/10.1023/A:1025401927023>
- [18] Langmuir, I. (1916) The Constitution and Fundamental Properties of Solids and Liquids. *Journal of the American Chemical Society*, **38**, 2221-2295.
<https://doi.org/10.1021/ja02268a002>
- [19] Dabhade, M.A., Saidutta, M.B. and Murthy, D.V.R. (2009) Adsorption of Phenol on Granular Activated Carbon from the Nutrient Medium: Equilibrium and Kinetic Study. *International Journal of Environmental Research*, **3**, 557-568.
- [20] Musumba, G., Nakiguli, C., Lubanga, C., Mukasa, P. and Ntambi, E. (2020) Adsorption of Lead (II) and Copper (II) Ions from Mono Synthetic Aqueous Solutions Using Bio-Char from *Ficus natalensis* Fruits. *Journal of Encapsulation and Adsorption Sciences*, **10**, 71-84. <https://doi.org/10.4236/jeas.2020.104004>
- [21] Akinhanmi, T.A., Edwin, A.O., Abideen, I.A., Peter, A. and Mayowa, J.I. (2020) Orange Peel as a Low-Cost Adsorbent in the Elimination of Cd (II) Ion: Kinetics, Isotherm, Thermodynamic and Optimization Evaluations.
<https://doi.org/10.21203/rs.3.rs-20604/v2>
- [22] Singanan, M. (2015) Biosorption of Hg (II) Ions from Synthetic Wastewater Using a Novel Biocarbon Technology. *Environmental Engineering Research*, **20**, 33-39.
<https://doi.org/10.4491/eer.2014.032>
- [23] Wen, H., Chen, J. and Zhang, J. (2020) Removal of Ciprofloxacin from Aqueous Solution by Rabbit Manure Biochar. *Environmental Technology*, **41**, 1380-1390.
<https://doi.org/10.1080/09593330.2018.1535628>
- [24] Dar, B., Taher, A., Wani, A. and Farooqui, M. (2013) Isotherms and Thermodynamic Studies on Adsorption of Copper on Powder of Shed Pods of *Acacia nilotica*. *Journal of Environmental Chemistry and Ecotoxicology*, **5**, 17-20.

- [25] Cruz-Lopes, L.P., Macena, M., Esteves, B. and Guiné, R.P.F. (2021) Ideal pH for the Adsorption of Metal Ions Cr^{6+} , Ni^{2+} , and Pb^{2+} in Aqueous Solution with Different Adsorbent Materials. *Open Agriculture*, **6**, 115-123. <https://doi.org/10.1515/opag-2021-0225>
- [26] Rabia, A., Muhammad, Y., Ahmad, M., Jaromír, K., Sidra, S., Sami, U., *et al.* (2020) Lead and Cadmium Removal from Wastewater Using Eco-Friendly Biochar Adsorbent Derived from Rice Husk, Wheat Straw, and Corn Cob. *Cleaner Engineering and Technology*, **1**, Article ID: 100006. <https://doi.org/10.1016/j.clet.2020.100006>
- [27] Zaib, M., Athar, M.M., Saeed, A., Farooq, U., Salman, M. and Makshoof, M.N. (2016) Equilibrium, Kinetic, and Thermodynamic Biosorption Studies of Hg (II) on Red Algal Biomass of *Porphyridium cruentum*. *Green Chemistry Letters and Reviews*, **9**, 179-189. <https://doi.org/10.1080/17518253.2016.1185166>
- [28] Sylwan, I., Runtti, H., Westholm, L.J., Romar, H. and Thorin, E. (2020) Heavy Metal Sorption by Sludge-Derived Biochar with Focus on Pb^{2+} Sorption Capacity at $\mu\text{g/L}$ Concentrations. *Processes*, **8**, Article 1559. <https://doi.org/10.3390/pr8121559>
- [29] Ahsan, M.A., Katla, S.K., Islam, M.T., Hernandez-Viezcas, J.A., Martinez, L.M., Díaz-Moreno, C.A., *et al.* (2018) Adsorptive Removal of Methylene Blue, Tetracycline, and Cr (VI) from Water Using Sulfonated Tea Waste. *Environmental Technology and Innovation*, **11**, 23-40. <https://doi.org/10.1016/j.eti.2018.04.003>
- [30] Li, J., Yu, G., Pan, L., Li, C., You, F., Xie, S., *et al.* (2018) Study of Ciprofloxacin Removal by Biochar Obtained from Used Tea Leaves. *Journal of Environmental Sciences*, **73**, 20-30. <https://doi.org/10.1016/j.jes.2017.12.024>
- [31] Marzbali, M.H. and Esmaili, M. (2017) Fixed Bed Adsorption of Tetracycline on a Mesoporous Activated Carbon: Experimental Study and Neuro-Fuzzy Modeling. *Journal of Applied Research and Technology*, **15**, 454-463. <https://doi.org/10.1016/j.jart.2017.05.003>
- [32] Beksissa, R., Tekola, B., Ayala, T. and Dame, B. (2021) Investigation of the Adsorption Performance of Acid-Treated Lignite Coal for Cr (VI) Removal from Aqueous Solution. *Environmental Challenges*, **4**, Article ID: 100091. <https://doi.org/10.1016/j.envc.2021.100091>
- [33] Sobh, M., Moussawi, M.-A., Rammal, W., Hijazi, A., Rammal, H., Reda, M., *et al.* (2014) Removal of Lead (II) Ions from Waste Water by Using Lebanese *Cymbopogon citratus* (Lemon Grass) Stem as Adsorbent *American Journal of Phytomedicine and Clinical Therapeutics*, **2**, 1070-1080.